

CHAPTER 2

**PREPARATION OF THE FILMS AND MEASUREMENT OF
PROPERTIES**

Chapter 2

PREPARATION OF THE FILMS AND MEASUREMENT OF PROPERTIES

2.1 Introduction

In this chapter, the preparation of the PbS nanocrystalline films and measurement of various properties have been discussed. Due to the merits of the chemical bath deposition (CBD) method, as discussed in the section 1.4 of chapter 1, we use this method for preparation of the films.

2.2 Preparation of the films

2.2.1 Selection of substrates

For the deposition of the PbS nanocrystalline films, microscopic glass slides have been selected as substrates for the following reasons [5]-

- (i) Inertness to chemicals used in the synthesis process
- (ii) Smoothness of the surface
- (iii) High electrical resistivity ($\sim 10^{15} \Omega\text{m}$)
- (iv) Good thermal stability at both high (upto 480K) as well as low (77K) temperature.
- (v) Easy availability and cost effectiveness.

2.2.2 Cleaning of substrates

The surface of the substrate is generally covered with various contaminants such as adsorbed water, dust, grease, oil etc. Proper cleaning of the substrates is required for obtaining good quality films. The procedure of substrate cleaning, after these are cut into required sizes, are outlined below-

- (i) At first, the substrates were washed with ordinary detergent solution and kept immersed in dilute HNO_3 for one night.

(ii) Then the substrates were washed thoroughly in distilled water and immersed in freshly prepared chromic acid for one hour.

(iii) After step (ii), the substrates were washed by distilled water, gently rubbed with wet filter paper swabs and again rinsed by double distilled water.

(iv) Lastly, the substrates were cleaned in an ultrasonic cleaner for 20 minutes.

(v) Now the substrates were put in a clean beaker nearly vertically and dried in a cleaned closed stainless still oven.

After cleaning and drying of the substrates following the above steps, these become ready for deposition of films.

2.2.3 Materials used for depositions

All reagents used are of analytical grade. These are

(i) Lead Nitrate (SRL, purity $\geq 99\%$)

(ii) Lead Acetate (SRL, purity $\geq 99\%$)

(iii) Thiourea (Merck, purity $\geq 99\%$),

(iv) Triethanolamine (Merck, purity $\geq 97\%$),

(v) Sodium Hydroxide (NICE Chemicals Pvt. Ltd. Purity $\geq 96\%$),

(vi) Zinc Chloride (sdfine-Chem Ltd. Purity $\geq 97\%$)

(vii) Ferric Chloride (sdfine-Chem Ltd. purity $\geq 97\%$).

Reagents were used as were purchased without further purification. Solutions were prepared in doubly distilled or deionized water manufactured by Stanbio Reagents (P) Ltd.

2.2.4 Formation of films by CBD method

The detailed procedure of formation of films on the substrates in a chemical bath is described in relevant chapters (Chapter 3, 4 and 5).

2.3 X-ray diffraction (XRD)

X-ray diffraction has been used to determine crystal structure of solids including size and shape of unit cell, preferred orientation in polycrystals, microstrain, identification of impurities etc.

2.3.1 Basic Principle[159]

A beam of x-ray passing through a crystal suffer scattering in all directions by the periodically arranged atoms of the crystal . In certain directions, the scattered rays interfere constructively resulting in enhancement of intensity, called diffraction maxima or peaks. The necessary condition for occurring constructive interference is the Bragg's law

$$n\lambda = 2d' \sin\theta \quad (2.1)$$

where n is the order of diffraction, λ is the wavelength of x-ray, d' is the spacing between atomic planes corresponding to Miller indices (hkl) and θ is angle of incidence of x-ray on the planes of atoms.

Eq. (2.1) may also be written as

$$\lambda = 2 (d'/n) \sin\theta \quad (2.2a)$$

$$\text{or } \lambda = 2 d \sin\theta \quad (2.2b)$$

where $d = (d'/n)$. Equations (2.2a and b) imply that n th order diffraction from (hkl) planes with spacing d' can be considered as first order diffraction from planes $(nh \ nk \ nl)$ with spacing $d = d'/n$. $(nh \ nk \ nl)$ are the Miller indices of the planes parallel to $(h \ k \ l)$ but

with $1/n$ th the spacing of the latter.

2.3.2 Determination of crystallite size from broadening of the diffraction peaks

Smaller crystallites cause broadening of the diffraction maxima. If the path difference between x-ray photons scattered by two consecutive planes of atoms (the first and the second plane, for example) differs only slightly from an integral number of wavelengths, then the plane of atoms scattering x-rays exactly out of phase with the photons scattered from the first plane will lie deep within the crystal. If the crystal is small, then this plane neutralising the scattering from the first plane may not exist. In that situation, the complete cancellation of all the scattered rays will not happen. As a result, the diffraction peak will get broadened [159]. Such broadening is always present in real diffraction experiment as the x-ray beam is neither perfectly parallel nor strictly monochromatic. The crystallite size (D) in the direction perpendicular to the (hkl) planes is given by Scherrer's formula [159]

$$D = \frac{0.9 \lambda}{\beta \cos \theta} \quad (2.3)$$

where β is the full width at half maximum of the peak resulting from the scattering from the (hkl) plane at the diffraction angle 2θ .

2.3.3 Microstrain

Due to existence of defects, a real crystal deviates from an ideal crystal. One of such defects is the small size of crystallites. The next common defects are the presence of subgrain structures and dislocations. In a real crystal, a grain is broken up into a number of tiny subgrains, slightly disoriented from each other. The angle of disorientation may vary from a very small value to as much as one degree, depending upon the crystal. If this angle is ϕ , then the diffraction of a parallel monochromatic

beam from a single crystal will occur not only at the angle of incidence θ , but at all angles between θ and $(\theta+\varphi)$. Due to the subgrain structure, the integrated intensity of the diffracted beam increases in comparison to the theoretically calculated value for a perfect crystal [159]. The subgrains are defined by the dislocations present in the subgrain boundaries.

If the strains vary from one grain to another or from one part of a grain to another part, then these are called microstrains. On the other hand, if the strains are uniform over large distances, these are called macrostrain. Strain affects the XRD peaks. Uniform strains shift the peak positions while non-uniform strains broaden the diffraction peaks [159]. The microstrains are calculated from the relation [160]

$$\varepsilon = \frac{\beta \cot \theta}{4} \quad (2.4)$$

where β and θ are the fwhm and the angle of incidence corresponding to XRD peak positions respectively.

If a plane of atoms lies only partway through a crystal, the edge of such plane is a defect in the form of a line which is called dislocation [161]. Plastic deformation in crystals occurs by *slip* (sliding of one part of the crystal over an adjacent one) and slip propagates by the motion of dislocations [24]. The line separating the slipped part of the material from the unslipped part is called dislocation line. Any appreciable plastic deformation is the result of a large number of dislocations sweeping across many slip planes. The rate of plastic flow is determined by the rate at which dislocation lines sweep through the slip planes i.e. the rate of plastic flow is proportional to the total length of all active dislocation lines and average velocity with which the elements of these lines move. Therefore the concept of 'dislocation density' has been introduced

which is defined as the length of dislocation lines per unit volume of the crystal [162]. The dislocation density (ρ) is given by the formula [163]

$$\rho = \frac{m \varepsilon}{aD} \quad (2.5)$$

where m is a constant having values 15, 24, 28 for (111), (220) and (311) planes respectively, ε is the microstrain, a is the lattice constant and D is the crystallite size.

2.3.4 Nelson-Riley plot [159]

Precise measurement of lattice parameter is very important for a number of studies. For example, the composition of a solid solution can be obtained from the measurement of lattice parameters. By observing the variation of lattice parameter with temperature, the thermal expansion coefficient can be determined.

The lattice parameter of a cubic lattice corresponding to the (hkl) plane is related to the interplanar spacing 'd' as

$$a = d \sqrt{h^2 + k^2 + l^2} \quad (2.6)$$

Differentiating (2.2) and using (2.6), it can be obtained

$$\frac{\Delta a}{a} = -\cot \theta \Delta \theta \quad (2.7)$$

Eq. (2.7) shows that error free values of lattice constant is obtained as $\theta = 90^\circ$ or $2\theta = 180^\circ$. But diffracted beams can not be observed at this angle. The best way to estimate the true value of lattice parameter is to plot its measured values against certain linear functions of θ and extrapolating it to $\theta = 90^\circ$. In finding the proper extrapolation function, various effects have to be considered which lead to errors in the measurement of θ . Also, the variation of these errors with the angle θ has to be found out.

When a diffractometer is used to measure d-spacings, the important sources of

systematic error in 'd' are-

- (i) Misalignment of the instrument.
- (ii) Use of a flat specimen instead of a specimen curved to conform to the focussing circle.
- (iii) Absorption in the specimen.
- (iv) Displacement of the specimen from the diffractometer axis which is considered the largest single source of error.
- (v) Vertical divergence of the incident beam.

The Nelson- Riley function

$$f(\theta) = [\cos^2\theta/\sin\theta + \cos^2\theta/\theta] \quad (2.8)$$

is an widely used extrapolation function.

Assuming this function to be appropriate, we can write

$$\frac{a - a_o}{a_o} = k \left[\frac{\cos^2 \theta}{\sin \theta} + \frac{\cos^2 \theta}{\theta} \right] \quad (2.9)$$

The extrapolation of the right hand side function which is the Nelson-Riley function $f(\theta)$ to $\theta=90^\circ$ gives $a=a_o$, the precise value of lattice parameter.

2.3.5 Corrections for instrumental broadening [164]

In addition to the broadening of the xrd peaks due to crystallite size and strain, there is additional broadening caused by instrumental effects such as slit width, wavelength spread, sample size, imperfect focussing and alignment etc. and it must be separated to get the correct breadth created due to small crystallite size and strain. The corrections for instrumental broadening can be done either by Stokes' method which derives the corrected profile by 'Convolution Analysis' or by a priori assumption of the nature of

such contributions. If β_o , β_i and β_t represent the observed, instrumental and true fwhm and if

(i) the contributions from instrument and the sample are described by Gaussian functions

$$\beta_o^2 = \beta_t^2 + \beta_i^2 \quad (2.10)$$

(ii) the contributions from instrument and the sample are described by Lorentzian functions

$$\beta_o = \beta_t + \beta_i \quad (2.11)$$

2.3.6 Indexing of the diffraction pattern and identification of phases [165]

(i) The interplanar spacing d_i and the relative intensities I_i of each peak are determined.
(ii) Then, these experimentally observed set of (d_i, I_i) are compared with standard data file of ICDD for indexing and identification of phases. For f.c.c structured PbS phase, the comparison is made with the standard data file ICDD PDF 78-1900.

2.3.7 Textured Coefficient

Quantitative information about the preferred orientation is given by the texture coefficient [100]

$$TC = \frac{I_m/I_s}{1/n \sum_1^n I_m/I_s} \quad (2.12)$$

where I_m is the measured intensity and I_s is the standard intensity of the peak corresponding to the (hkl) plane and n is the number of diffraction peaks considered. TC is maximum for the preferred plane of growth and is greater than unity. If $TC \leq 1$, the crystallites are considered to be randomly oriented.

2.3.8 Standard XRD peaks of bulk PbS

The standard xrd peak positions of bulk PbS are obtained by plotting the relative intensities against the angle of diffraction 2θ (degree) as given by the ICDD PDF No. 78-1900. As per the standard data file, the unit cell of the material is face centred cubic (f.c.c) with lattice constant of 5.936 Å. The peak positions are obtained at $2\theta = 26.019^\circ$, 30.133° , 43.137° , 51.07° , 53.517° , 62.649° , 69.017° , 71.077° , 79.096° and 84.962° corresponding to (111), (200), (220), (311), (222), (400), (331), (420), (422) and (511) planes respectively. (200) is the plane with highest relative intensity, next comes the (111) plane. The ratio of the relative intensities between (200) and the (111) planes is 1.05.

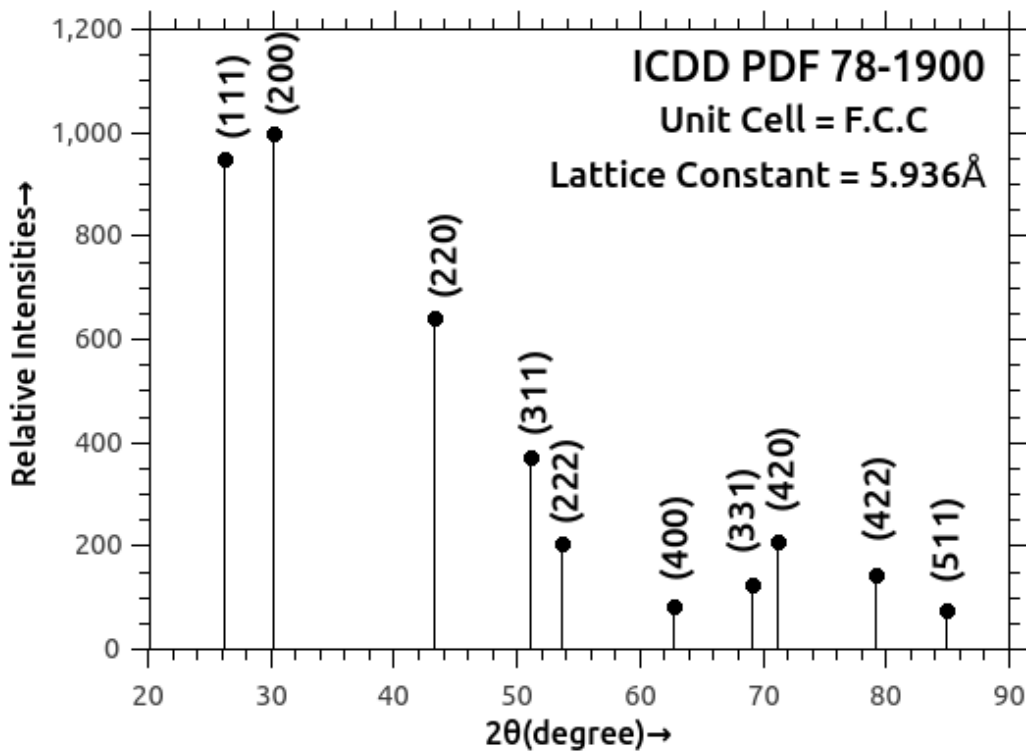


Fig. 2.1: Standard xrd peaks of bulk PbS

2.4 Scanning Electron Microscope (SEM) [1]

Scanning Electron Microscope or simply SEM provides topographical (surface features) and morphological (shape and size distribution) information as well as chemical composition of the material and their relative amount (% weight and % atomic contents) near the surface of the material. Its resolve upto a few nanometers and magnification can be adjusted from ~10 to over 3,00,000.

In a typical SEM, the surface of the sample is scanned by a beam of electrons of very fine spot size of ~ 5 nm and energy ranging from a few hundred eV to 50 KeV, with the help of deflecting coils. As the electrons penetrate the surface, three types of interactions may take place resulting in the emission of electrons and photons from the sample. These interactions are briefly described below-

(i) Inelastic scattering: When a high energy primary electron interacts with an atom in the material, it may undergo inelastic scattering with atomic electron of the target in which the primary electron transfers a part of its energy to the atomic electron. If the energy transferred is sufficient, the atomic electron will be emitted from the sample. The emitted electron is called secondary electron if its' energy is less than 50 eV. The images formed by the secondary electrons are known as the secondary electron image.

(ii) Elastic scattering: When a high energy primary electron interacts with an atom in the material, it may undergo elastic scattering with atomic nucleus of the target. Then the scattered electron will have the same energy as the incident electron. The backscattered electrons are elastically scattered. The probability of backscattering increases with the atomic number of the target material. The images formed by the backscattered electrons are known as backscattered electron image.

(iii) *X-ray photon or Auger electron emission*: In another interaction, the primary electron may eject a core electron from a target atom. The excited atom will relax to its ground state by emitting either a characteristic X-ray photon or an Auger electron, both of which have been used for chemical characterization of the sample. The chemical compositions of the material can be determined by measuring the energies of the emitted X-ray photon and the Auger electron. The emitted X-ray is used in the Energy Dispersive X-ray Spectroscopy (EDX) and the Auger electron is used in the Auger Electron Spectroscopy (AES).

2.5 Transmission Electron Microscope (TEM) [1]

Transmission electron microscope or TEM provides morphological, structural and crystallographic information of an object at magnifications ranging from 50 to 10^6 and resolution upto 1 nm and below. Here, electrons are accelerated to 200 keV and above and projected onto a thin specimen (thickness smaller than 200 nm) by means of the condenser lens system and penetrate the sample thickness either deflected or undeflected. The kind of information obtained is determined by the scattering process experienced by the penetrating electron. Elastic scattering gives rise to diffraction pattern and the inelastic scattering at heterogeneities such as grain boundaries, dislocations, defects, density variations etc. leads to a spatial variation in the intensity of the transmitted electrons. By changing the strength of the intermediate lens, the switching between imaging and the diffraction mode can be done.

Selected area electron diffraction (SAED) determines the crystal structure of individual nanomaterials and of different parts of a sample. The crystal structure is determined by the same procedure as used in XRD. In SAED, the condenser lens is

defocused to produce parallel illumination at the specimen and a selected area aperture is used to limit the diffracting volume.

Since electron scattering is highly sensitive to the target element, like SEM, EDX can be developed in TEM also.

High-resolution transmission electron microscopy (HRTEM) is an imaging mode of the TEM that allows for direct imaging of the atomic structure of the sample. At present, the highest point resolution realised in phase contrast TEM is around 0.5 Å. At these small scales, individual atoms of a crystal and its defects can be resolved. [166]

2.6 Raman Spectroscopy [1,5]

Raman spectroscopy is a nondestructive spectroscopic technique used as a tool for molecular fingerprinting and to identify changes in chemical bonds. When a monochromatic radiation is allowed to pass through a substance, the incident photon excites the chemical bond to a higher energy state. Most of the energy would be re-radiated at the same frequency as that of the incident photon in the form of scattered beam. This scattering at the frequency of the incident photon is called Rayleigh scattering. When a small portion of the energy is transferred to excited vibrational modes, the Raman scattering is called Stokes scattering. The frequency of the Stokes line is lower than Rayleigh line. Existing exciting vibrations may add their energies to the incident beam by coupling with the latter. Then the resulting Raman line appears at frequencies higher than the Rayleigh line. Such scattering is called anti-Stokes scattering. The Stokes and anti-Stokes lines are mirror images on opposite sides of the Rayleigh line. But the Stokes line is more intense than the anti-Stokes line. The Raman shift represents the phonon frequencies of the substance. In Raman spectroscopy, the

“*optical phonon*” mode corresponds to high frequency lattice vibration while “*acoustic phonon*” mode corresponds to much lower frequency lattice vibration.

2.7 Optical Absorption [167]

The absorption spectrum of a material gives information about the band structure. In the absorption process, a photon of known wavelength excites an electron to a higher energy state. When a monochromatic beam is passed through a semiconductor, the intensity of the transmitted radiation decreases due to absorption by the substance. By studying the absorption, all possible electronic transitions can be discovered and distribution of states can be determined. Absorption is expressed in terms of absorption co-efficient $\alpha(h\nu)$ defined as the relative rate of decrease in light intensity $I(h\nu)$ of frequency ν along its propagation path (assumed x axis):

$$\alpha = \frac{1}{I(h\nu)} \cdot \frac{d[I(h\nu)]}{dx} \quad (2.13)$$

There are various types of absorption processes which are outlined below-

(i) Fundamental absorption

Fundamental absorption refers to the valence band to conduction band transition characterized by rapid rise in absorption. Fundamental absorption can be used to determine the energy gap of the semiconductor. The absorption coefficient is proportional to the probability for transition from the initial state to the final state, density of the electrons in the initial state and density of the available final states. The fundamental transitions are categorized as *allowed direct transitions* (momentum of the electron 'p' is conserved and the transition probability is independent of photon energy) , *forbidden direct transitions* (direct transitions at $p=0$ is forbidden, but allowed at $p \neq 0$), *indirect transitions* (both energy and momentum of the electron change and the total

momentum is conserved via phonon interaction) and *transitions between band tails* (responsible for exponential absorption edge).

(ii) Higher energy transitions

Direct transitions from valence band to conduction band can occur at almost all points in the momentum space except those forbidden by selection rules. Again, away from the conduction band minimum, the valence and the conduction band are separated by higher energies. Hence, the direct transitions which takes place at a point different from the valence band maximum involve energies greater than the band gap. Moreover, existence of subbands in both conduction and valence bands also allow higher energy transitions.

(iii) Exciton absorption

The pair of a free hole and a free electron attracted by Coulomb interaction is called exciton. The exciton can move through the crystal as single particle. Its formation usually appears as narrow peaks in the absorption edge of direct band gap semiconductors and as steps in the absorption edge of indirect band gap semiconductors. In the former, the free exciton forms when

$$h\nu = E_g - E_x \quad (2.14)$$

where E_g is the band gap and E_x is the binding energy of the exciton. At the momentum $p=0$, this appears as a sharp peak in the absorption spectrum which broadens with temperature.

In indirect gap semiconductors, phonon participation is required to conserve momentum. Hence the increase in absorption co-efficient is obtained at

$$h\nu = E_g - E_x \pm E_p \quad (2.15)$$

E_p is the phonon energy, + sign for transition with phonon emission and – sign for the

transition with phonon absorption. A number of steps in the absorption edge can be obtained depending upon the combination of phonons participating in the transition.

(iv) Isoelectronic traps

Isoelectronic centers are formed when one atom of the crystal is substituted by another of the same valence. These centers can bind an exciton. Interactions between closely spaced isoelectronic centers results in new set of energy levels for the bound excitons.

(v) Transition between a band and an impurity level

The transition between a neutral donor and the conduction band or between the valence band and the neutral acceptor can occur by the absorption of a low energy photon which have energy at least equal to the ionization energy of the impurity. Typically, this energy corresponds to the far infrared region of the electromagnetic spectrum. On the other hand, the transition between the valence band and an ionized donor or between an ionized acceptor and the conduction band occurs at photon energies given by

$$h\nu > E_g - E_i \quad (2.16)$$

where E_i is the impurity level. The transitions between an impurity and a band is characterized by a shoulder in the absorption spectrum below the band gap. The absorption coefficients for transitions involving the impurity level covers a much smaller range than transitions between valence and conduction bands because the density of impurity states is much lower than the density of states in the bands. In practice, due to transitions involving tails of states, it is very difficult to resolve shallow impurities from the background of absorption. Deep levels can contribute a step in the absorption spectrum, when the ionization energy of the impurity is large compared to the width of the absorption edge.

2.8 Transmittance, Reflectance and Absorbance of a thin film

An electromagnetic wave passing through a thin film of thickness t gets attenuated because of absorption of radiation by the material of the film and reflection from the surface as well as the film-substrate interface. If I_0 is the intensity of the incident radiation and I is that of the transmitted radiation then the transmittance (T) of the film is defined as [167]

$$T = I/I_0 \approx (1-R)^2 e^{-\alpha t} \quad (2.17)$$

where R is the reflectance and α is the absorption co-efficient. The absorbance (A) of the film is defined as [8]

$$A = \log \left[\frac{(1-R)^2}{T} \right] \quad (2.18)$$

The absorbance is related to the absorption co-efficient by (using eqs. 2.17 and 2.18)

$$\alpha = \frac{2.303 A}{t} \quad (2.19)$$

2.9 Urbach Energy

The exponential behaviour of absorbance below the band gap gives rise to tail in the absorption spectrum. This is due to the electronic transition between localized states which tails off into the energy gap. These states arise due to various defects present in the film. The dependence of absorbance (A) on wavelength (λ) along the tail is represented by the Urbach relation [168]

$$A(\lambda) = A_0 \exp \left(\frac{hc}{E_u \cdot \lambda} \right) \quad (2.20)$$

where E_u represents the width of the tails of the localized states in the forbidden band

called 'Urbach energy', A_0 is a constant, h is Plank's constant and c is the speed of light in free space. The reciprocal of slope of the linear regression of ' $\ln A$ ' vs. ' $1/\lambda$ ' gives the value of E_u by the following relation [169]

$$E_u = \frac{1240}{\text{Slope}} \text{ (eV)} \quad (2.21)$$

2.10 Direct and indirect band gap

The direct and indirect band gaps can be determined from the relation [110]

$$(\alpha h\nu)^n = P(h\nu - E_g) \quad (2.22)$$

where $E = h\nu$ is the energy of the absorbed photon, E_g is the band gap and P is a constant. For direct allowed transitions $n=2$ and for indirect allowed transition $n= 1/2$. Since α is proportional to the absorbance A for a given film, the above relation can also be written as

$$(AE)^n = Q(E - E_g) \quad (2.23)$$

Q is another constant. The extrapolation of the linear part of $(AE)^n$ vs. E curve to $(AE)^n = 0$ axis gives the direct and indirect band gap for $n=2$ and $1/2$ respectively.

There is also another method called the "derivative method" for determination of direct band gap. According to this method, the direct band gap is that energy at which the slope of the absorbance vs. energy is the maximum i.e. the energy at which

$$\frac{dA}{dE} = \text{maximum} \quad (2.24)$$

The background of the derivative method can be understood as follows:

Eq. (2.19) represents the absorption spectrum below the band gap. This equation is characterized by a positive curvature (rising slope). Absorption above the band gap is due to band-to-band transition and is governed by the equation [170]

$$A = \frac{B 2 \pi \sqrt{E_b}}{1 - \exp \left[-2 \pi \sqrt{\frac{E_b}{(h \nu - E_g)}} \right]} \quad (2.25)$$

where B is a constant, E_b is the lowest state exciton binding energy, ν is the frequency of incident radiation and E_g is the band gap. This equation is characterized by a negative curvature (decreasing slope). The band gap, which represents the onset of band-to-band transition, is the energy at which the curvature changes from positive to negative or, equivalently, the energy at which the slope of the absorption spectrum is maximum [171, 172]. This method was used for determination of band gap by Hernn´dez-Borja et.al [123] and Zak et.al [173].

2.11 Complex refractive index

The velocity of propagation of an electromagnetic wave in a medium is given by [167]

$$v = \frac{c}{n_c} \quad (2.26)$$

where c is the velocity of the electromagnetic wave in vacuum and n_c is the complex refractive index of the medium given by

$$n_c = n - ik \quad (2.27)$$

where the real part 'n' is called the refractive index and the imaginary part 'k' is called the extinction coefficient of the medium. The extinction coefficient represents the attenuation of electromagnetic radiation per one vacuum wavelength travel within the substance and is given by [169]

$$k = \frac{\alpha \lambda}{4 \pi} \quad (2.28)$$

The refractive index 'n' of the medium is given by

$$n = \frac{1+R}{1-R} + \sqrt{\frac{4R}{(1-R)^2} - k^2} \quad (2.29)$$

where R is the reflectance of the medium.

2.12 Photoluminescence (PL)

In photoluminescence, the sample is excited by means of photons of definite wavelength and the luminescence emitted during de-excitation is used to assess qualitative and sometimes, quantitative information about chemical composition, structure, impurities, kinetic process and energy transfer [1].

The semiconductor which gains energy from the photon, promotes an electron from the valence band to conduction band. The system then undergoes a non-radiative internal relaxation by interaction with rotational and vibrational modes and the excited electron moves to a more stable excited state such as the conduction band minimum. After a characteristic lifetime in the excited state, the electron will return to the ground state emitting luminescence. The wavelength of the emitted light is longer than that of the incident light. PL is called “fluorescence” if the characteristic lifetime of emission is of the order of submicrosecond and “phosphorescence” if the lifetime is 10^{-4} -10 s [1].

High excitation energies above the band gap can be most effective for luminescence studies of bulk materials, but in case of nanoparticles, the efficiency of luminescence decreases at high excitation energies. Nonradiative relaxation can short circuit the luminescence at these high energies [2]

2.13 Conductivity of the films

The conductivity (σ) of the film has been determined from the relation [9]

$$\sigma = \frac{L}{RBt} \quad (2.30)$$

where L is the spacing between the electrodes, B is the breadth in between the contacts, t is the thickness of the film and R is the resistance of the film as determined from the slope of the current-voltage characteristics. The factors affecting the conductivity of the films are [1]:

(i) *Phonons, surface and defects*: Collision of conduction electrons with vibrating atoms displaced from their equilibrium lattice positions are the source of the phonon contribution to the electrical conduction, which increases linearly with temperature. Lattice defects such as impurity, grain boundary, dislocations, vacancies etc. cause electron scattering by locally disrupting the periodic electric field of the crystal. The contributions from the lattice defects are independent of temperature. When the critical dimension of the thin film is smaller than the electron mean free path, the motion of electrons will be interrupted through collision with the surface. Inelastic collision with the surface reduces the conductivity.

(ii) *Quantum size effect* : Reduction of characteristic dimension below the electron de-Broglie wavelength leads to widening of the band gap. Such broadening of band gap results in decrease of conductivity.

(iii) *Quantum transport*: Three types of quantum transport occur in small devices and materials-

(a) *Ballistic conduction*: It occurs when the length of the conductor is smaller than the

electron mean free path. Each transverse waveguide mode contributes $12.9 \text{ (k}\Omega\text{)}^{-1}$ to the total conductance. Another important aspect of ballistic transport is that no energy is dissipated in the conduction and no elastic scattering occurs.

(b) Coulomb blockade: Coulomb blockade occurs when the contact resistance is larger than the resistance of the nanostructure and when the total capacitance of the object is so small that adding a single electron requires significant charging energy.

(c) Tunneling conduction: If two extremely closely spaced conductors are separated by a very thin insulating layer, tunneling of electrons between the conductors may take place under the action of an electric field.

(iv) *Microstructure*: Electrical conductivity may change due to the formation of ordered microstructure when the size is reduced to nanometer scale.

2.14 Thickness measurement

Gravimetric method is a reliable method for the determination of the thickness of the film. In this method, a highly sensitive electronic microbalance is used. The thickness (t) of the film is given by [174]

$$t = \frac{W}{\rho A} \quad (2.31)$$

where W is the mass of the deposited film, ρ is the density and A is the area of the film.